Critical Role of Adsorption Equilibria on the Determination of Surface-Enhanced Raman Enhancement

Ashish Tripathi,[†] Erik D. Emmons,[†] Augustus W. Fountain, III,[‡] Jason A. Guicheteau,[‡] Martin Moskovits,[*,§] and Steven D. Christesen[*,‡]

[†]Leidos, Chemical Biological Solutions Directorate, 3465A Box Hill Corporate Center Drive, Abingdon, Maryland 21009, United States, [‡]Research and Technology Directorate, Edgewood Chemical Biological Center, Aberdeen Proving Ground, Aberdeen, Maryland 21010-5424, United States, and [§]Department of Chemistry and Biochemistry, University of California, Santa Barbara, California 93106, United States

ABSTRACT Surface-enhanced Raman spectroscopy (SERS) is a useful technique for probing analyte–noble metal interactions and determining thermodynamic properties such as their surface reaction equilibrium constants and binding energies. In this study, we measure the binding equilibrium constants and Gibbs free energy of binding for a series of nitrogen-containing aromatic molecules adsorbed on Klarite substrates. A dual Langmuir dependence of the SERS intensity on concentration was observed for the six species studied, indicating the presence of at least two different binding energies. We relate the measured binding energies to the previously described SERS enhancement value (SEV) and show that the SEV is proportional to the traditional SERS enhancement factor *G*, with a constant of proportionality that is critically dependent on the adsorption equilibrium constant determined from the dual Langmuir isotherm. We believe the approach described is generally applicable to many SERS substrates, both as a prescriptive approach to determining their relative performance and as a probe of the substrate's affinity for a target adsorbate.

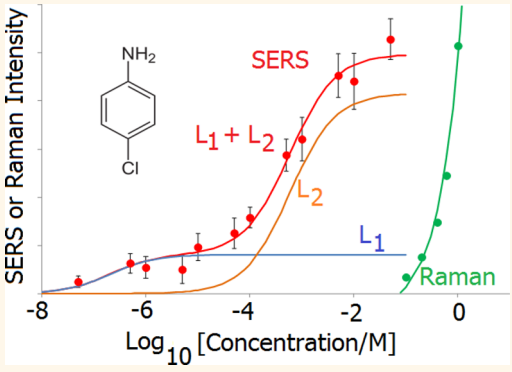

KEYWORDS: SERS · equilibrium constant · binding energy · enhancement factor · Langmuir isotherm

The strengths of surface–molecule interactions vary greatly. The process of chemisorption is often marked by the formation of strong covalent or dative bonds between the surface and a molecular analyte (*e.g.*, thiol molecules bound to noble metal surfaces), whereas physisorption is usually characterized by weak bonds between the molecule and the surface (*e.g.*, aniline bound to gold). In addition to the nature of the bond between the surface and the adsorbed analyte molecule, the solvent can also play an important role. If the affinity between the solvent and analyte is strong, the analyte–surface reaction may be slowed and the equilibrium may be shifted. Many different experimental techniques have been used to study adsorption of molecules, and surface-enhanced Raman spectroscopy (SERS) has proved valuable for examining the interactions of molecules with noble metals.[1−4]

In 1916, Irving Langmuir proposed a model describing adsorption on surfaces which included a function now known as the Langmuir isotherm, connecting the surface coverage to the concentration of the adsorbate in the ambient medium.[5,6] The reaction kinetic equations leading to molecule–surface equilibrium are given by

$$S^* + P \leftrightarrows SP \qquad (1)$$

where S^* is an unoccupied surface site, P is an unadsorbed analyte molecule, and SP is a bound analyte/surface-site pair. The equilibrium constant for the reaction, K, can be written as

$$K = \frac{[SP]}{[S^*][P]} \qquad (2)$$

where the brackets indicate concentrations. Langmuir was able to derive a relation between the fractional coverage of surface sites occupied, θ, and the concentration, C, of analyte molecules in solution (or,

* Address correspondence to steven.d.christesen.civ@mail.mil, moskovits@chem.ucsb.edu.

Received for review October 15, 2014 and accepted December 17, 2014.

Published online December 17, 2014
10.1021/nn5058936

alternatively, in a vapor) as follows:

$$\theta = \frac{KC_S}{1 + KC_S} \quad (3)$$

allowing K to be determined experimentally from the concentration dependence of θ. Three assumptions are inherent in establishing the Langmuir isotherm relation:[7]

(a) The forward reaction (adsorption) rate is directly proportional to the vapor pressure of analyte in the gas phase or molar concentration of analyte in the liquid phase, C_S, and to the number of unoccupied adsorption sites. The backward reaction (desorption) rate is directly proportional to the number of occupied adsorption sites.

(b) For C_S to refer to the initial partial pressure or solution concentration of the adsorbate, the partial pressure or molar concentration of the analyte must remain effectively constant during the adsorption process. In practice, this means that a large enough volume of solution must be used so that the number of adsorbent molecules in solution is much larger than the number of adsorption sites. This also ensures that the forward rate of reaction is directly proportional to the number of unoccupied adsorption sites at a given analyte concentration.

(c) The surface must be exposed to the solution for a long enough time to allow the system to achieve equilibrium at the concentration used. For very low concentrations, the time might be several days.

Previously, we showed that a waiting period of seven half-lives was sufficient to achieve at least 99% of full surface coverage when the substrate was immersed in an adsorbate solution of 5×10^{-7} M; specifically, the rate constant for binding of thiophenol to gold (Klarite) at 5×10^{-7} M (7 mL volume) at pH 6 and 26 °C was determined to be 1.67×10^{-3} s^{-1}, corresponding to a reaction half-life of ~410 s.[8] Seven half-lives, ~2900 s, were found to be sufficient to reach 99% of the molecule's equilibrium coverage on Klarite. This length of time is not experimentally onerous, and since the reaction rate is given by the rate constant multiplied by the concentration, the wait time for solution more concentrated than 5×10^{-7} M would be even shorter. However, adsorption out of lower concentration solution would scale as the inverse of the concentration. So for adsorption out of a 5×10^{-8} M solution, the wait time would grow to 29 000 s, and out of a 5×10^{-9} M solution, the wait time would require 290 000 s, that is, ~81 h. Likewise, one must be mindful of the volume of solution one offers to the substrate so as to ensure that the adsorption process does not seriously reduce the concentration of the adsorbate in solution.

In carrying out this study, we once again measured the time evolution of the SERS signal to ensure that the results we present are consistent with adsorption equilibrium. This is illustrated by the results we obtained using isoquinoline adsorbing on Klarite whose SERS spectra recorded at a concentration of 5×10^{-7} M (13.5 mL volume) and 23 °C are shown in Figure 1a. The temporal profiles of the three most prominent Raman spectral features of isoquinoline (530, 780, and 1385 cm^{-1}) are plotted in Figure 1b, from which the half-lives of the reaction determined from the time evolution of these three bands assuming first-order kinetics were determined to be 430, 370, and 410 s, respectively. These values were obtained by fitting the intensity *versus* time curves to a function rising to a constant value as unity minus an exponentially decreasing function. Because the estimated error in the half-life is ~40 s, we consider the three half-lives to

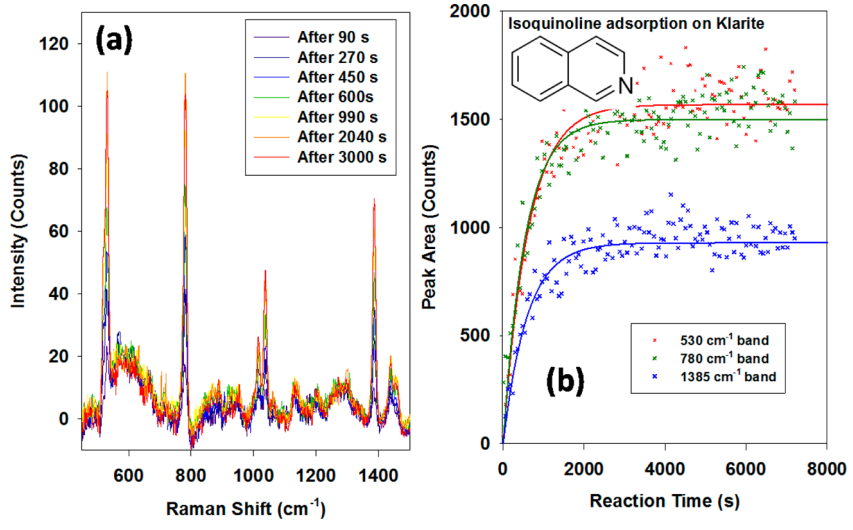

Figure 1. (a) Raman spectra for the adsorption of isoquinoline onto Klarite out of 13.5 mL of 5×10^{-7} M solution at 23 °C. (b) Time evolution of three Raman bands of isoquinoline reacting with Klarite. The substrate was continuously exposed to the laser during this time period.

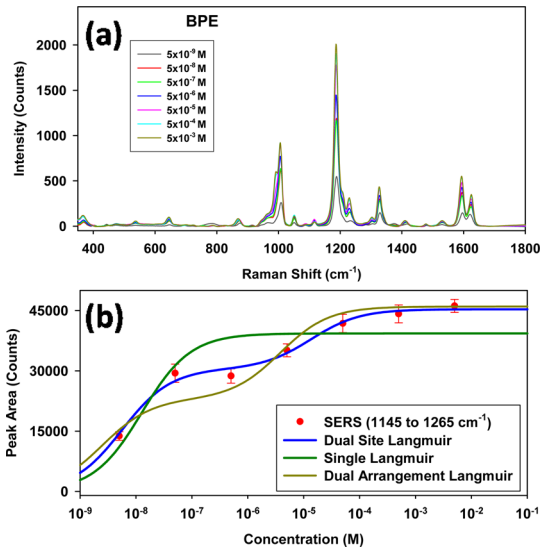

Figure 2. BPE SERS spectra on a Klarite substrate. (a) Average SERS spectra at various BPE concentrations. (b) Peak area of the 1186 cm^{-1} line as a function of concentration.

be essentially equal, with an average value of 403 s. In Figure 2b, seven half-lives (*i.e.*, ~2800 s) does indeed correspond to a time at which the SERS signal has reached a value at least 99% of the maximum value. For adsorption of isoquinoline out of a 5×10^{-9} M solution, we, therefore, estimate that 99% of full coverage would require 282 000 s, that is, ~79 h. This "seven half-life corrected for concentration" rule was used to ensure equilibrium for each of the analytes studied.

In addition to providing sufficient time, one also must ensure that the adsorption process does not significantly reduce the concentration of the adsorbate in solution. Once again, this issue arises primarily at very low concentration as discussed previously,[8] where, for example, we estimated that 1.7×10^{14} molecules of thiophenol are needed to form a full self-assembled monolayer (SAM) on a Klarite substrate. In a 5×10^{-9} M solution, this number of molecules is contained in approximately 60 mL. By immersing the substrate in ~1 L of 5×10^{-9} M solution, the formation of a full monolayer would reduce the concentration by approximately ~4% (an acceptably small amount).

In the present work, the fraction of surface sites occupied by analyte molecules, θ, is calculated from the SERS intensity by the following expression:

$$\theta = \frac{I_{C_S}}{I_{max}} \tag{4}$$

where I_{C_S} is the SERS peak area of an analyte-specific Raman line at an analyte molar concentration of C_S and I_{max} is the SERS peak area of the same Raman line when a complete SAM is formed. Combining eqs 3 and 4, we obtain

$$I_{C_S} = I_{max}\left(\frac{KC_S}{1 + KC_S}\right) \tag{5}$$

Equation 5 is used to fit the Raman peak area *versus* analyte concentration data with I_{max} and the equilibrium constant, K, as the fitting parameters.

Estimating the Free Energy of Adsorption. The equilibrium constant is related to the Gibbs free energy of adsorption (ΔG) as follows.

$$\Delta G = -RT \ln(K) \tag{6}$$

where R is the ideal gas constant and T is the temperature.[7] This allows the free energy of adsorption to be determined by fitting the SERS data to eq 5. If ΔG is measured as a function of temperature, the enthalpic and entropic contributions to ΔG can also be determined from[9,10]

$$\Delta G = \Delta H - T\Delta S \tag{7}$$

RESULTS AND DISCUSSION

Six nitrogen-based aromatic compounds of varied structure (isoquinoline, 1,2-bis(4-pyridyl)ethylene (BPE), pyridine, pyrazine, 4-chloroaniline, and aniline) were selected for the study in order to present the substrate with species having varied chemical affinities for gold. The first four of these molecules are aza-arenes, with at least one nitrogen atom substituted for a carbon atom in the aromatic ring(s). They differ in the number of rings, the bridging between the rings, and the position and number of nitrogen atoms. The last two are aromatic amines, with NH_2 groups attached to the rings. The Langmuir isotherms were obtained by immersing the Klarite substrates in large enough volumes containing more than a sufficient number of analyte molecules and for durations of time sufficient to satisfy the conditions discussed above.

Consider the adsorption of BPE on Klarite. A 0.1 M BPE stock solution in ethanol was prepared and serially diluted from 5×10^{-2} to 5×10^{-9} M using ultrapure water (18.3 MΩ·cm) as diluent. After each immersion period, the Klarite substrate was transferred to a Petri dish and 7 mL of the solution used during the immersion period was added to the Petri dish to maintain the equilibrium and to completely cover the substrate. A Raman spectral map consisting of a 6×6 grid of points was then acquired. This procedure was repeated for each concentration used.

Figure 2a shows the average spectra recorded at each concentration. Figure 2b shows the peak area of the 1186 cm^{-1} Raman band as a function of concentration (red circles with 99% confidence error bars). The data were fit to a Langmuir isotherm (eq 5) with the maximum peak area as a multiplier, as shown by the green curve in Figure 2b. The equilibrium constant was determined to be 7.8×10^7, corresponding (at room temperature) to a free energy of adsorption of −44.8 kJ/mol. The regression coefficient, r^2, was 0.7445, indicating a poor fit, as is obvious on visual

inspection. The data appear to suggest that there are two plateaus: one at lower concentrations and other at higher concentrations, rather than one, as eq 5 predicts. Two plateaus imply a dual "arrangement" of BPE molecules on the substrate. Langmuir predicted such complications and offered two simple models to describe dual (or multiple) surface equilibria.[6]

In the first model, Langmuir assumed that there may be more than one type of "elementary space" making up the substrate. Each of these elementary spaces allows the adsorbent to bind in a different orientation and/or density. Let β_1, β_2, β_3, *etc.* be the fractions representing each of these elementary spaces. The expression equivalent to eq 3 describing such a situation becomes

$$\theta = \frac{\beta_1 K_1 C_S}{1 + K_1 C_S} + \frac{\beta_2 K_2 C_S}{1 + K_2 C_S} + etc. \quad (8)$$

with the constraint

$$\beta_1 + \beta_2 + \ldots = 1$$

For BPE, the different elementary spaces can be viewed as BPE adsorbing in different modes of orientation (potentially differing in adsorption energy) and/or density.[1,12−17] The data presented in Figure 2 suggest that two types of elementary spaces exist. In this case, eq 8 reduces to a dual Langmuir isotherm form:

$$\theta = \frac{\beta_1 K_1 C_S}{1 + K_1 C_S} + \frac{\beta_2 K_2 C_S}{1 + K_2 C_S} \quad (9)$$

Combining eqs 5 and 9 yields the following equation:

$$I_{C_S} = I_{max}\left(\frac{\beta_1 K_1 C_S}{1 + K_1 C_S} + \frac{\beta_2 K_2 C_S}{1 + K_2 C_S}\right) \quad (10)$$

We will refer to the model described by eq 10 as the dual-site Langmuir isotherm. Fitting the dependence of peak area of 1186 cm^{-1} Raman band as a function of concentration (red circles in Figure 2b) to eq 7 results in the solid blue line in Figure 2b. The values of I_{max}, β_1, β_2, K_1, and K_2 were used as fitting parameters. The regression coefficient, r^2, was 0.9873, and K_1, K_2, and their respective free energy values were determined to be 1.8×10^8, 7.3×10^4, and −46.8 and −27.6 kJ/mol, respectively.

In the second model, Langmuir assumed that there may be more than one molecule occupying the same elementary space, resulting in a higher packing density at higher concentrations.[12] Let θ_1, θ_2 ... θ_n be the fractions of elemental spaces that are blank, occupied by 1, 2 ... *n* number of molecules. In this case, eq 3 can be modified to the following form:

$$\theta = \frac{K_1 C_S + 2K_1 K_2 C_S^2 + 3K_1 K_2 K_3 C_S^3 \quad \ldots}{1 + K_1 C_S + K_1 K_2 C_S^2 + K_1 K_2 K_3 C_S^3 \quad \ldots} \quad (11)$$

In the case of BPE, up to two molecules can be viewed as adsorbing on the same elementary space. Thus, eq 8 reduces to the following dual-molecule single-site Langmuir isotherm form:

$$\theta = \frac{K_1 C_S + 2K_1 K_2 C_S^2}{1 + K_1 C_S + K_1 K_2 C_S^2} \quad (12)$$

Combining eqs 4 and 12 yields the following equation:

$$I_{C_S} = I_{max}\left(\frac{K_1 C_S + 2K_1 K_2 C_S^2}{1 + K_1 C_S + K_1 K_2 C_S^2}\right) \quad (13)$$

We will refer to the model described by eq 13 as the dual-arrangement Langmuir isotherm. Fitting the concentration dependence of the peak area of the 1186 cm^{-1} Raman band to eq 13 (red circles in Figure 2b) results in the solid gold line (Figure 2b). The values of I_{max}, K_1, and K_2 were used as fitting parameters. The coefficient of regression, r^2, was 0.903, a better fit than that provided by a single Langmuir but not as good as the dual-site Langmuir. The values of K_1, K_2, and corresponding free energy values were determined to be 4.0×10^8, 2.6×10^5, and −48.8 and −30.7 kJ/mol, respectively. While the dual-site Langmuir and dual-arrangement Langmuir isotherms fit the data adequately well, they do not explain the mechanism driving the dual-adsorption process. The two processes may result from the structural heterogeneity of the Klarite substrate, which is composed of multiple inverted nanopyramids. The molecular binding and SERS enhancement of the BPE molecules adsorbed at the edges as opposed to the faces of the inverted pyramids might differ. Alternatively, the molecular binding mode might change as the adsorption density increases. It is unlikely, however, that the observed isotherm shape is due to the adsorption of multiple analyte layers at the higher concentrations. The SERS intensity is known to drop off very rapidly as the molecule−substrate distance increases. This would result in much lower SERS intensities for the second monolayer than for the first, which is not what is observed. In fact, the height of the second step in the dual isotherm is large, in some cases higher than the first step.

The process described above was repeated for pyridine, pyrazine, isoquinoline, aniline, and 4-chloroaniline (please see the accompanying Supporting Information). For each of these compounds, the dual-site Langmuir model provides the best fit, although in some cases, it is not significantly better than the dual-arrangement model. In summary, the adsorbate binding mechanism cannot be conclusively determined from the goodness of the fits. A single Langmuir, however, is without doubt insufficient to account for the experimental results. Table 1 lists the values of fitting parameters obtained from the three Langmuir models for all the compounds.

SERS Enhancement and the Langmuir Equilibrium Constant. It is reasonable to expect that the intrasubstrate differences in binding energy for the same analyte and the differences in binding energy for different analytes will have an effect on the chemical enhancement

TABLE 1. Estimated Equilibrium Constants of Binding (M^{-1}) of the Listed Analytes to Klarite Substrate and the Corresponding Free Energies of Binding (kJ/mol) at 23 °C

Molecule	Structure	Single Langmuir		Dual Site Langmuir					Dual Arrangement Langmuir		
		K (ΔG)	R^2	K_1 (ΔG_1)	K_2 (ΔG_2)	β_1	β_2	R^2	K_1 (ΔG_1)	K_2 (ΔG_2)	R^2
BPE	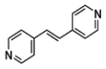	7.8×10^7 (-45)	0.74	1.8×10^8 (-47)	7.3×10^4 (-28)	0.67	0.33	0.99	4.0×10^8 (-49)	2.6×10^5 (-31)	0.90
Pyridine		8.8×10^3 (-22)	0.91	1.5×10^7 (-41)	3.1×10^3 (-20)	0.22	0.78	0.98	1.7×10^5 (-30)	1.1×10^3 (-17)	0.95
Isoquinoline		5.5×10^6 (-38)	0.83	2.6×10^7 (-42)	3.5×10^4 (-26)	0.59	0.41	0.98	4.7×10^7 (-43)	6.2×10^4 (-27)	0.97
Pyrazine		1.4×10^4 (-23)	0.86	2.7×10^5 (-31)	4.0×10^2 (-15)	0.42	0.58	0.99	1.5×10^5 (-29)	2.8×10^2 (-14)	0.98
Aniline		1.9×10^1 (-7.3)	0.96	1.7×10^4 (-24)	1.5×10^1 (-6.6)	0.09	0.91	0.97	1.0×10^2 (-11)	6.3 (-4.6)	0.93
4-Chloroaniline	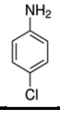	4.1×10^3 (-20)	0.93	4.8×10^6 (-38)	1.7×10^3 (-18)	0.16	0.84	0.99	2.3×10^4 (-25)	3.7×10^2 (-15)	0.97

component of the SERS enhancement, depending on how we measure that enhancement. The normal definition of SERS enhancement is the SERS enhancement factor, *G*:

$$G = \frac{I_S N_R}{I_R N_S} \tag{14}$$

where I_S and I_R are, respectively, the SERS intensity due to N_S "participating" molecules and the ordinary Raman intensity due to N_R of the same molecules in solution. However, *G* has proved difficult to calculate reliably as a consequence of the fact that it depends on at least one, and often more than one, hard to determine parameter. Most often, it is N_S that cannot be accurately determined because many of the following parameters are not known with confidence: the surface area of the nanostructured surface, the dose, and the cleanliness of the surface, which might already have competing species occupying an indeterminate fraction of the surface. Additionally, as described above, the surface concentration of the analyte will follow an isotherm, which is a function of the analyte's concentration in solution and on the surface's chemical affinity for that molecule.

For measurements of analytes in solution or in the vapor phase, *G* is a poor measure of the sensitivity of the SERS substrate because it does not take into account the equilibrium established between the ambient environment and the surface. It is simply a measure of the enhancing power of the substrate assuming one knows the coverage, which is often assumed to be full coverage, with little supporting evidence. To ameliorate these issues when using *G* as a measure of substrate efficacy, Guicheteau *et al.*[11] developed a wholly prescriptive approach resulting in a SERS figure of merit that was called the SERS enhancement value (SEV), which gauges the benefit of SERS as an analytical tool over ordinary Raman for a given SERS substrate and a given adsorbate molecule. This measure corrects operationally for the aforementioned difficulty of determining N_S and also for the spatial inhomogeneity of the enhancement of many SERS substrates. The spatial inhomogeneity may result in the "sacrifice" of a large fraction of the adsorbed molecules at weakly enhancing sites. The SEV is also dependent on the analyte's Gibbs free energy of binding through the Langmuir isotherm equilibrium constant.

The SEV,[11] which for brevity we will call *F*, was defined as the ratio of the two analyte concentrations C_R and C_S, producing the same Raman and SERS intensities, the former being the concentration of the analyte in solution in the absence of the SERS substrate and the latter being the concentration of the analyte in the solution from which the analyte was adsorbed (at equilibrium) onto the SERS substrate. It is clear that there are an infinite number of pairs of concentrations that would satisfy this condition. Guicheteau *et al.* used receiver operating characteristic (ROC) curves to identify the SERS intensity that provided a 90% probability of detection (PD) and a 10% probability of false alarm. That intensity was then used to determine C_R and C_S.[11] An alternative approach will be used here inspired by the ROC curves to determine C_R and C_S by measuring Langmuir isotherms and replacing the 90% PD with the

SERS signal intensity that is 90% of the maximum SERS value. This approach has the benefit that F is defined entirely in terms of measurable and definable factors, such as concentrations, without having to make assumptions regarding the number of molecules that contribute to the SERS or ordinary Raman intensities.

Issues relating to computing the SERS enhancement and the limitations of its application in chemical analysis have been discussed previously,[3,18,19] most thoroughly by Etchegoin and Le Ru.[18] Here we will develop the relationship between F and the SERS enhancement factor, G, and determine the system variables that must be considered when comparing the two measures. We will then show the effect of the equilibrium constant (and, therefore, the binding energy) on the measurement of both F and G.

Restricting our analysis to a SERS substrate that is dosed with a molecular adsorbate out of solution and comparing this result to what is measured for the same molecule by ordinary Raman spectroscopy in solution, eq 14 may be rewritten as

$$G = \frac{I_S C_R V}{I_R n_S A} \tag{15}$$

where V is the focal volume which produces the normal Raman signal, A is the focal area, the area that contains the n_S molecules that we associate with the measured SERS signal, C_R is the analyte concentration in the solution from which the ordinary Raman spectrum was measured, and n_S is the number of adsorbed molecules per unit area producing the SERS signal.

Assuming that n_S is the surface concentration when the substrate is in equilibrium with a solution of the adsorbate at solution C_S, we relate n_S and C_S using the Langmuir isotherm described previously in eq 5:

$$n_S = \frac{KC_S n_{max}}{1 + KC_S} \tag{16}$$

where n_{max} is the maximum number of adsorbate molecules that (on average) can occupy a unit area of surface on the SERS substrate. Substituting eq 16 into eq 15 yields

$$G = \frac{I_S}{I_R} \frac{C_R V(1 + KC_S)}{KC_S n_{max} A} \tag{17}$$

One can define pairs of concentrations C_S^0 and C_R^0 at which $I_S = I_R$. That is, when the SERS substrate is immersed in a solution in which the analyte concentration is C_S^0 and equilibrium is allowed to be established, one obtains a SERS intensity I_S for a given Raman band which is equal to the intensity I_R of the same band measured in the ordinary Raman spectrum of the analyte in a solution in which its concentration is C_R^0. If so, then the quantity $F = C_R^0/C_S^0$ functions as a measure of the analytical value of SERS over ordinary Raman. For example, if by using SERS one can obtain a Raman signal by exposing a SERS substrate to an analyte with concentration $C_S^0 = 10^{-8}$ M (having achieved adsorption equilibrium) while in solution the same (ordinary) Raman intensity is achieved when $C_R^0 = 10^{-3}$ M, then $F = 10^5$. Using these definitions, the $I_S = I_R$ condition, and eq 16, one can relate G to F as follows:

$$G = \frac{FV(1 + KC_S^0)}{Kn_{max}A} \tag{18}$$

in which the SERS and the ordinary Raman intensities do not appear.

Following the work of Guicheteau *et al.*,[11] one can define a more useful and prescriptive version of eq 18 by specifying an appropriate criterion for selecting the value of C_S^0 to use. In doing so, we will ignore two potential complications: the first is the possibility that a SERS hot spot also has some special affinity for the adsorbate (either chemically or optical-field-induced), which might result in more intense SERS signals from the first molecules to adsorb on the surface as compared to those that adsorb later on; that is, we will assume that the adsorbate adsorbs on the SERS substrate's surface in a manner that is independent of that site's SERS enhancement. We will also ignore the decrease in SERS intensity per molecule on approaching monolayer coverage due to the depolarizing effect of neighboring adsorbate on a given molecule. This depolarizing effect results in a SERS intensity at full monolayer coverage that is actually a little less than for partial (but near full) monolayer coverages, as first pointed out by Murray and Bodoff[20] and reported by other groups.[21] Ignoring these effects, we assume that the SERS intensity will be proportional to N_S, so that when the SERS intensity is a factor $\alpha \leq 1$ of its maximum value then $n_S = \alpha n_{max}$. Defining F_α as the value of F measured according to eq 18 and evaluating the value of C_S^0 by substituting $n_S = \alpha n_{max}$ in eq 16, one obtains the following equation relating F_α to G:

$$F_\alpha = G\frac{(1 - \alpha)Kn_{max}A}{V} \tag{19}$$

Several properties of F_α are obvious from eq 19. First, F_α is proportional to the Raman enhancement factor, G, although, in general, numerically different from it. F_α depends critically on several molecular and instrumental parameters and (trivially) on the choice of α. Chief among these parameters are the focal volume, V, and the focal area, A, which depend on the magnifying power of the lens used to focus the excitation laser and on the numerical aperture used to collect the laser light (which in many instruments is accomplished using the same lens) and also on the longitudinal and lateral sizes of the aperture. A large focal volume, for example, will result in a smaller value of F_α, and a molecule that has a greater affinity for the SERS substrate (*i.e.*, a greater value of K) will produce a larger value of F_α than one with a lower affinity. Finally,

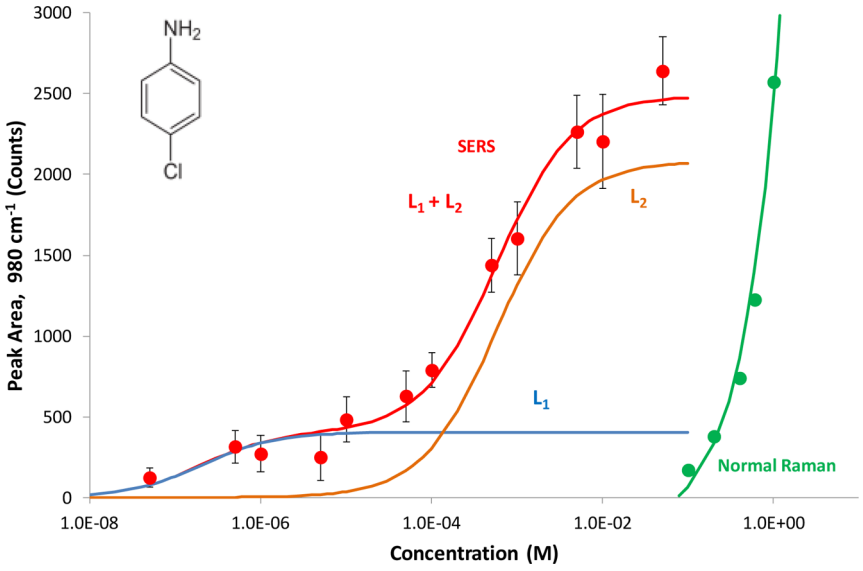

Figure 3. SERS and normal Raman peak areas for 4-chloroaniline. The circles represent the data; the red curve is the dual Langmuir fit to the data, and L_1 and L_2 are the components of the dual-site Langmuir fit.

molecules characterized by small values of n_{max} will produce lesser values of F_α, all else being equal.

Values of F_{90} (*i.e.*, F values evaluated at α = 90%) were derived for the six adsorbate molecules (BPE, aniline, 4-chloroaniline, isoquinoline, pyrazine, and pyridine) by measuring their SERS intensities at various concentrations, thereby determining the adsorption isotherm of each as described above. The normal Raman spectrum of each of the species was also measured as a function of the concentration in aqueous solution. As an example, the measured SERS isotherm and ordinary Raman peak intensity dependence on concentration for 4-chloroaniline are shown in Figure 3. The Raman intensities are for a single peak, and the values at each concentration are the average of 16 spectra measured at different locations on the Klarite substrate. Similar to the other analytes measured, the SERS intensity for 4-chloroaniline as a function of concentration produced a function that fit the dual-site Langmuir isotherm described by eq 10 (red curve in Figure 3). As discussed previously for BPE, this implies that there are two distinct sites for that molecule with differing chemical affinities. While the dual-arrangement isotherm fit does not fit the data as well as the dual-site isotherm does, we cannot completely rule out the possibility that the molecule changes orientation as a function of coverage, resulting in two saturation regimes as a function of concentration.[1,12−17]

We will continue our discussion in terms of the dual-site model only. The calculated values of the free energy of adsorption indicate that the surface possesses at least two classes of adsorption sites, with site 1 forming a more stable surface bond than site 2. The ΔG values vary between −47 and −24 kJ/mol for site 1 and between −28 and −7 kJ/mol in site 2. The relative occupation probability in sites 1 and 2 at equilibrium as indicated by the β_1/β_2 ratio (Table 1) does not always favor the site with the lower value of the adsorption free energy, reflecting the complex nature of the equilibrium which includes dynamical processes involving molecules in the two adsorption sites and their counterparts in solution, as well as molecular exchanges between the two adsorption sites to which both entropic and enthalpic effects contribute. Nevertheless, the larger values of β_1 roughly correspond to the more negative values of ΔG_1 with a couple of outliers.

TABLE 2. Measured Values F_{90} and Calculated *Gn* for the Six Species Studied[a]

molecule	$F1_{90}$	*calculated *Gn*	$F2_{90}$	*calculated *Gn*	**calculated *Gn*
4-chloroaniline	450000	5.6×10^{19}	160	5.6×10^{19}	5.7×10^{19}
aniline	2500	2.0×10^{19}	6	1.9×10^{20}	2.0×10^{20}
isoquinoline	510000	1.2×10^{19}	480	8.2×10^{18}	2.0×10^{19}
pyrazine	1300	6.2×10^{18}	5	8.8×10^{18}	1.5×10^{19}
pyridine	260000	1.0×10^{19}	190	3.7×10^{19}	4.8×10^{19}
BPE	16000000	5.4×10^{19}	6900	5.5×10^{19}	8.2×10^{19}
average		2.6×10^{19}		6.0×10^{19}	7.0×10^{19}
		(2.3×10^{19})		(6.9×10^{19})	(6.7×10^{19})

[a] Calculated using eq 18 (*), and eq 15 (**) where $I_S = I_{max}$ and $n_S = n_{max}$ and expressed to two significant digits. The following values were assumed: $V = 2.2 \times 10^{-9}$ mL; $A = 2.2 \times 10^{-8}$ cm^2. The numbers in parentheses are the standard deviations of the calculated *Gn* values.

The measured SEV (F_{90}) values, extracted from the measured isotherms (Table 2), range from ~5 for pyrazine and aniline to ~1.6×10^7 for BPE, and the respective K (M^{-1}) values (Table 1) ranged from 15 (aniline) to 1.8×10^8 (BPE). The four aza-arenes were found to have the largest values of K, implying a high affinity for the gold surface, likely due to the fact that these molecules can π-bond by lying flat on the surface. The higher values of K for BPE and isoquinoline,

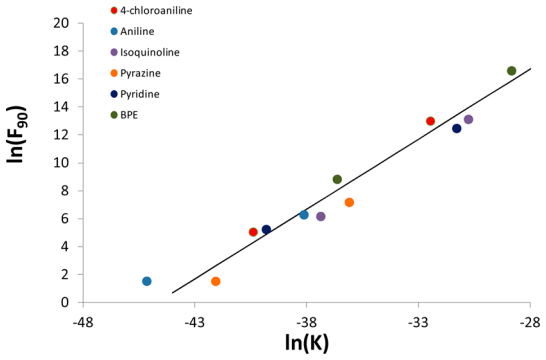

Figure 4. A ln−ln plot of the measured values of F_{90} *vs K* illustrating their proportionality as predicted for these two quantities (eq 19). There are two points for each compound corresponding to the dual Langmuir fits to the data. The blue line corresponds to a best fit, forcing a slope of unity. The intercept corresponds to the quantity defined by eq 20.

which can bond through both rings, is consistent with this conjecture (although we recognize that several other factors may also be at play here). The molecules with lowest affinity are the anilines, whose amine group may prevent them from lying flat on the surface, thereby hindering the establishment of a good π-bond.

The values of F_{90} are plotted in Figure 4 as a function of K (a ln−ln plot is used to accommodate the wide range of K values). The good fit between the fitted line (with a forced slope of unity) and the measured points (bearing in mind that data corresponding to the two plateaus were fit to the same line) suggests that the above analysis has considerable validity. It also shows that F_{90} is a good proportional measure of G for a given molecule when comparing the relative merits of various SERS substrates. Referring to eq 19, a ln−ln plot of F_α *versus* K (Figure 4) yields an intercept of

$$\ln\left(\frac{G(1-\alpha)n_{max}A}{V}\right) \qquad (20)$$

A least-squares fit to the data listed in Table 1 (K_S for dual-site Langmuir) and Table 2 (F_S) yields an intercept value of 44.7, which corresponds to a value for the quantity in parentheses in eq 20 of 4.1×10^{19} molecules/cm^3. G is generally presumed to be a characteristic property of the Klarite substrate, and if robust values of V, A, and n_{max} are available, the SERS enhancement can be determined from F *via* eq 19. The quantity A might be estimated from the diffraction-limited size of the illuminating laser beam and V from the numerical aperture of the microscope objective.[22] While the diffraction-limited spot size (2.2×10^{-8} cm^2) is a good estimate for A, determining V is more complicated. The standard formulas for focal volume yield an estimate $\sim$5 μm for the focal volume length. However, an increasing Raman signal is observed for liquid sample thicknesses out to $\sim$0.5 mm. We have therefore decided to use this latter value for the focal volume length, resulting in a value of $V = 2.2 \times 10^{-9}$ mL. The value of n_{max} is the least straightforward quantity to estimate, largely on account of the heterogeneity of many SERS substrates both in terms of their SERS enhancement and with respect to their adsorption affinity toward a target analyte. For example, the value of n_{max} would be reduced if the analyte is reluctant to adsorb on a significant portion of the substrate's surface either intrinsically or because some sites on the surface are already occupied by other species. Conversely, its value would be increased if the surface's roughness factor is greater than unity, thereby permitting a larger number of molecules to occupy a unit projected area.

The fit in Figure 4 would indicate that the quantity $G \times n_{max}$ (hereafter denoted as Gn), and not G, is a fundamental property of the substrate alone and is independent of the analyte. If G is the enhancement per molecule, then Gn can be considered the average enhancement per unit area of the substrate. From eq 20, we calculate a value of 2.5×10^{19} for Gn. It is gratifying to note that the value of Gn computed using eq 15 and the conditions $I_S = I_{max}$ and $n_S = n_{max}$, for each of the analytes used in this study (last column in Table 2), is in close agreement with this value.

Equation 19 also provides a method of calculating Gn for individual analytes. In this case, we get two values for each analyte: one for each F_α/K pair obtained from the dual Langmuir isotherm fit (third and fifth column in Table 2). All of the Gn values agree to within about a factor of 30 even though two different methods were used for their calculation. The Gn values averaged over all analytes are also close to that obtained from the intercept of the ln(F) *versus* ln(K) plot described above. In addition, although the values for the K vary from 6.3 to 4.0×10^8 (Table 1), the Gn values calculated using eq 19 differ by less than a factor of 30.

If we assume an average value of 1.9×10^{14} molecules/cm^2 used in previous estimates[8] of G for Klarite, one obtains a value of $G \cong 1.3 \times 10^5$ from the intercept in Figure 4. This value lies in the 10^4 to 10^6 enhancement range claimed for Klarite by its manufacturer.

CONCLUSIONS

SERS continues to hold great promise as a flexible sensor platform due in part to its large per molecule sensitivity and because the plasmon resonance of a nanostructured metallic substrate can be tuned over a wide range of laser excitation wavelengths, allowing the development of a SERS sensor to capitalize on the vast diversity of spectroscopic systems with respect to lasers, spectrographs, and detectors. However, the literature suggests that the relative enhancement for a given molecule is often acutely substrate-dependent. A key consideration often neglected in SERS measurements is the adsorption affinity of a molecule toward the substrate surface, which can range from weak

physical adsorption to the formation of strong covalent or dative bonds. In addition, since of necessity SERS substrates are nanostructured and therefore often surface-structurally complex, they would also often be surface-chemically heterogeneous. The mechanism(s) driving these equilibrium reactions requires further study in order to determine *a priori* which molecules can be analytically detected using a given SERS substrate. It is also important to establish experimental conditions that allow for a realistic calculation of the enhancement factor and/or understand the limitations of that estimate when ideal conditions are not met. For all the molecules investigated in the present study, a single Langmuir isotherm model was found insufficient in describing the observed equilibrium. A complex equilibrium with two binding energies was observed for each of the analytes.

Although the SERS enhancement factor, G, has gained near universal acceptance as a substrate's figure of merit, we believe that the development of the SERS enhancement value accomplishes two important goals. First, by measuring the equilibrium constant for a series of molecules, the SERS substrate's response can be quantified with fewer assumptions and arguably less error. Also from knowledge of the equilibrium constant, the sensor's performance could be estimated prescriptively. This could lead to greater predictability of SERS activity of molecules, which is a critical factor when developing sensors or sensing strategies for a wide range of analytes. Second, the SEV produces an unbiased analysis of substrate performance, permitting direct comparison of the relative merits of various substrates produced by disparate substrate manufacturing techniques and often with parameters that are nearly impossible to estimate correctly. The analysis we present provides a simple formula for deriving the SERS enhancement from the SEV and indicates clearly what parameters need to be known accurately in order to calculate a meaningful SERS enhancement value (and, if unknown, what quantitative assumptions are being made). While the SEV is fundamentally tied to the analyte's equilibrium constant, our analysis indicates that the product of the normally defined SERS enhancement factor times the maximum number of molecules per unit area that can bind to the surface ($G \times n_{max}$) is a fundamental property of the substrate alone.

EXPERIMENTAL METHODS

Materials. Pyridine, aniline, 4-chloroaniline, isoquinoline, pyrazine, and BPE were purchased from Sigma-Aldrich and used without further purification. Solutions were prepared in deionized water in the range of 5×10^{-9} to 0.1 M concentrations. All the experiments were performed at room temperature (23 °C) with the SERS substrate immersed in the analyte solution. Commercially available gold SERS substrates (Klarite, KLA-312, Renishaw Diagnostics Ltd., UK) were used for this work. The substrates provide adequately strong and reproducible SERS enhancement with 785 nm excitation.[8,11] The topography of the Klarite SERS substrates was reported previously.[8] The 7 mL of solution in which the substrate was immersed during all of the SERS measurements fully covered the substrate with a 2.4 mm thick layer of liquid above the surface of the substrate. Evaporation was minimized by covering the Petri dish except for a small hole where the laser beam illuminated the surface.

Raman Microscopy. Raman measurements were performed with a JASCO NRS-3200 dispersive Raman microscope system operating at 785 nm excitation with approximately 4 mW power incident on the sample. A 10× microscope objective was used both to focus the laser on the substrate and to collect the Raman scattered light. The relatively modest laser power and magnification were used to minimize laser-induced heating of the substrate. These factors, combined with the continuous stirring of the temperature-regulated analyte solution, adequately mitigate local heating of the spot on the substrate illuminated by the laser. Because the bottom of the microscope objective was above the surface of the liquid, an immersion objective was not needed. A diagram of the experimental setup was shown in a previous article.[8] The Raman scattered light was dispersed with a 600 grooves/mm diffraction grating (blazed at 750 nm), and a spectrometer entrance slit width of 100 μm was used to obtain a spectral resolution of approximately 8 cm^{-1}. Raman spectra were acquired with 25 s of integration time and averaged over three co-additions. The Raman scattered light was detected with a thermoelectrically cooled CCD camera (Andor). Rayleigh scattered light was suppressed with a notch filter (Semrock). Raman spectral mapping of the substrate was performed by selecting a 36 location grid on the substrate, in a rectangular 6 × 6 format, and obtaining Raman spectra at each location. The spectra shown in this article were baseline-corrected using a fourth-order polynomial fit for display purposes only.

Conflict of Interest: The authors declare no competing financial interest.

Supporting Information Available: Additional spectra, isotherms for the full set of the molecules examined, and a table of the concentrations, immersion times, and volumes used to determine the isotherms. This material is available free of charge *via* the Internet at http://pubs.acs.org.

Acknowledgment. M.M. wishes to acknowledge support for this work by the Institute for Collaborative Biotechnologies through Contract No. W911NF-09-D-0001 from the U.S. Army Research Office. We would also like to thank Mr. Philip Wilcox for his assistance with MATLAB programming. We would like to recognize the U.S. Army for funding of this work through ECBC's Surface Science Initiative (PE 0601102A VR9). The opinions, interpretations, conclusions and recommendations are those of the authors and are not necessarily endorsed by the United States Government.

REFERENCES AND NOTES

1. Biggs, K. B.; Camden, J. P.; Anker, J. N.; Duyne, R. P. V. Surface-Enhanced Raman Spectroscopy of Benzenethiol Adsorbed from the Gas Phase onto Silver Film over Nanosphere Surfaces: Determination of the Sticking Probability and Detection Limit Time. *J. Phys. Chem. A* **2009**, *113*, 4581–4586.
2. Wang, H.; Levin, C. S.; Halas, N. J. Nanosphere Arrays with Controlled Sub-10-nm Gaps as Surface-Enhanced Raman Spectroscopy Substrates. *J. Am. Chem. Soc.* **2005**, *127*, 14992–14993.
3. Le Ru, E. C.; Etchegoin, P. G. *Principles of Surface-Enhanced Raman Spectroscopy and Related Plasmonic Effects*; Elsevier: Amsterdam, 2009.

4. Stiles, P. L.; Dieringer, J. A.; Shah, N. C.; Van Duyne, R. P. Surface-Enhanced Raman Spectroscopy. *Annu. Rev. Anal. Chem.* **2008**, *1*, 601–626.
5. Langmuir, I. The Constitution and Fundamental Properties of Solids and Liquids. Part I. Solids. *J. Am. Chem. Soc.* **1916**, *38*, 2221–2295.
6. Langmuir, I. The Adsorption of Gases on Plane Surfaces of Glass, Mica and Platinum. *J. Am. Chem. Soc.* **1918**, *40*, 1361–1403.
7. Atkins, P. W. *Physical Chemistry*; W.H. Freeman and Company: New York, 1999.
8. Tripathi, A.; Emmons, E. D.; Christesen, S. D.; Fountain, A. W.; Guicheteau, J. A. Kinetics and Reaction Mechanisms of Thiophenol Adsorption on Gold Studied by Surface-Enhanced Raman Spectroscopy. *J. Phys. Chem. C* **2013**, *117*, 22834–22842.
9. Karpovich, D. S.; Blanchard, G. J. Direct Measurement of the Adsorption-Kinetics of Alkanethiolate Self-Assembled Monolayers on a Microcrystalline Gold Surface. *Langmuir* **1994**, *10*, 3315–3322.
10. Schessler, H. M.; Karpovich, D. S.; Blanchard, G. J. Quantitating the Balance Between Enthalpic and Entropic Forces in Alkanethiol/Gold Monolayer Self Assembly. *J. Am. Chem. Soc.* **1996**, *118*, 9645–9651.
11. Guicheteau, J. A.; Farrell, M. E.; Christesen, S. D.; Fountain, A. W.; Pellegrino, P. M.; Emmons, E. D.; Tripathi, A.; Wilcox, P.; Emge, D. Surface-Enhanced Raman Scattering (SERS) Evaluation Protocol for Nanometallic Surfaces. *Appl. Spectrosc.* **2013**, *67*, 396–403.
12. Carron, K. T.; Hurley, L. G. Axial and Azimuthal Angle Determination with Surface-Enhanced Raman-Spectroscopy—Thiophenol on Copper, Silver, and Gold Metal-Surfaces. *J. Phys. Chem.* **1991**, *95*, 9979–9984.
13. Haehner, G.; Woell, C.; Buck, M.; Grunze, M. Investigation of Intermediate Steps in the Self-Assembly of *n*-Alkanethiols on Gold Surfaces by Soft X-ray Spectroscopy. *Langmuir* **1993**, *9*, 1955–1958.
14. Schreiber, F. Structure and Growth of Self-Assembling Monolayers. *Prog. Surf. Sci.* **2000**, *65*, 151–256.
15. Schreiber, F.; Eberhardt, A.; Leung, T. Y. B.; Schwartz, P.; Wetterer, S. M.; Lavrich, D. J.; Berman, L.; Fenter, P.; Eisenberger, P.; Scoles, G. Adsorption Mechanisms, Structures, and Growth Regimes of an Archetypal Self-Assembling System: Decanethiol on Au(111). *Phys. Rev. B* **1998**, *57*, 12476–12481.
16. Schwartz, D. K. Mechanisms and Kinetics of Self-Assembled Monolayer Formation. *Annu. Rev. Phys. Chem.* **2001**, *52*, 107–137.
17. Whelan, C. M.; Smyth, M. R.; Barnes, C. J. HREELS, XPS, and Electrochemical Study of Benzenethiol Adsorption on Au(111). *Langmuir* **1999**, *15*, 116–126.
18. Le Ru, E. C.; Blackie, E.; Meyer, M.; Etchegoin, P. G. Surface Enhanced Raman Scattering Enhancement Factors: A Comprehensive Study. *J. Phys. Chem. C* **2007**, *111*, 13794–13803.
19. Moskovits, M. Persistent Misconceptions Regarding SERS. *Phys. Chem. Chem. Phys.* **2013**, *15*, 5301–5311.
20. Murray, C. A.; Bodoff, S. Depolarization Effects in Raman Scattering from Cyanide on Silver-Island Films. *Phys. Rev. B* **1985**, *32*, 671–688.
21. Blue, D.; Helwig, K.; Moskovits, M. Diffusion of Ethylene and Xenon in Thin Pyrazine Layers. *J. Phys. Chem.* **1989**, *93*, 8080–8089.
22. Lewis, I. R.; Edwards, H. G. M. *Handbook of Raman Spectroscopy*; Marcel Dekker: New York, 2001; p 153.